Journal of Biosciences and Medicines, 2024, 12, 407-432
https://www.scirp.org/journal/jbm
ISSN Online: 2327-509X
ISSN Print: 2327-5081

Differential Expressed Genes in ECV304 Endothelial-Like Cells Infected with Herpes Simplex Virus Type 2

Yuqi Xu[1], Meiling Gong[1], Wenling Zheng[2], Wenli Ma[2], Yali Zhang[3], Xiaoyang Mo[4], Huanying Zheng[5], Changwen Ke[5], Meilan Liu[1], Diaodiao Shi[1], Hui Zhang[1,6], Haiquan Zhao[1*], Yaqiong Ye[1*]

[1]School of Animal Science and Technology, Foshan University, Foshan, China
[2]Institute of Genetic Engineering, Southern Medical University, Guangzhou, China
[3]Department of Clinical Laboratory Science, Guiyang Medical College, Guiyang, China
[4]The Center for Heart Development, Key Lab of National Education Ministry, College of Life Sciences, Hunan Normal University, Changsha, China
[5]Guangdong Province Center of Disease Control Virology Section, Guangzhou, China
[6]College of Animal Science and Technology, Jiangxi Agriculture University, Nanchang, China
Email: *cn874462@163.com,*fszhaohq@163.com

How to cite this paper: Xu, Y.Q., Gong, M.L., Zheng, W.L., Ma, W.L., Zhang, Y.L., Mo, X.Y., Zheng, H.Y., Ke, C.W., Liu, M.L., Shi, D.D., Zhang, H., Zhao, H.Q. and Ye, Y.Q. (2024) Differential Expressed Genes in ECV304 Endothelial-Like Cells Infected with Herpes Simplex Virus Type 2. *Journal of Biosciences and Medicines*, **12**, 407-432.
https://doi.org/10.4236/jbm.2024.1211034

Received: October 15, 2024
Accepted: November 23, 2024
Published: November 26, 2024

Abstract

Herpes simplex virus (HSV), the viral agent causing human genital herpes, recurs easily and poses significant harm to patients, while also being associated with atherosclerosis (AS). Currently, no effective therapy or vaccine exists to combat HSV. Previous studies have demonstrated the presence of HSV and its DNA in AS-diseased tissue, yet the precise pathogenesis of HSV involvement remains unclear. To investigate the genetic mechanism of HSV-induced vascular endothelial injury and AS, a type of human umbilical vein endothelial cells (ECV-304 cells) cultured in vitro were infected with herpes simplex virus type 2 (HSV-2). The effect of HSV-2 on differential gene expression in ECV304 cells was investigated by gene microarray technology during the early stages of infection. The results revealed a total of 462 differentially expressed genes, with 318 genes exhibiting up-regulated expression and 144 genes showing down-regulated expression. Furthermore, bioinformatics analysis revealed that all 462 differentially expressed genes were implicated in 237 distinct biological processes. Notably, 79 of these biological processes demonstrated statistically significant differences ($P < 0.05$), encompassing critical functions such as protein synthesis, ribosome biogenesis and assembly, as well as DNA and mRNA metabolism. Our findings have unveiled the differentially expressed genes of HSV-2 in ECV304 cells during infection, offering crucial

insights into the pathogenic mechanisms underlying HSV-2 invasion of endothelial cells and the pathobiology of AS.

Keywords

HSV-2, ECV304 Cells, Microarray

1. Introduction

Herpes simplex virus (HSV) belongs to the *α* subfamily of herpesviridae [1]. Human infections caused by the herpes simplex virus (HSV) can be categorized into two distinct types: HSV-1 and HSV-2 [2] [3]. Herpes Simplex Virus type 2 (HSV-2) is implicated not only in genital and neonatal infections but also in the pathogenesis of cervical cancer and atherosclerosis (AS) [4] [5]. Furthermore, HSV-2 infection exhibits a synergistic relationship with Human Immunodeficiency Virus (HIV) infection [6]. Prior research has demonstrated the presence of HSV antigens and their corresponding DNA sequences at sites of lesions in AS, specifically within vascular smooth muscle cells (SMCs) and endothelial cells (ECs) [7]. The prevalence of positive serum HSV antibodies is markedly elevated in patients with AS. This evidence suggests that HSV infection may play a significant role in the initiation and progression of AS. The detection of HSV DNA within the vascular wall of AS further indicates a potential association between HSV infection and the development of atherosclerosis.

To date, the detailed pathological mechanisms of HSV involvement in AS, in particular the relationship of HSV with EC and SMC, the major cells of the vessel wall, *in vitro* is unclear. The effect of the virus on target cells *in vitro* could reflect the direct effect of the virus on cells *in vivo*. Studying the biological effects of HSV infection on vascular endothelial cells *in vitro* is important to elucidate the mechanisms of HSV induction.

DNA expression profiling microarrays are designed to monitor the presence or expression of various genes in samples [8] [9]. Thus, by analyzing these data, we can determine whether the tested specimen is infected with the pathogen and the extent of the infection. Microarray technology has also been used to study the effects of other viruses on ECV304 endothelial cells [10] [11]. Due to the expensive equipment and the complexity of the experiments, there are no reports on the effect of HSV on the gene expression profile of endothelial cells.

In this study, our aim is to identify the differentially expressed genes in endothelial cells induced by HSV-2, and to explore the genetic mechanisms by which HSV-2 causes vascular endothelial injury, dysfunction, and atherosclerosis. We used a high-density microarray containing 18,000 genes to compare the gene expression profiles of HSV-2-treated ECV-304. This allowed us to determine the differential expression of HSV-2-induced endothelial cell genes and to explore the genetic mechanisms by which HSV-2 causes vascular endothelial injury and dysfunction and AS.

2. Materials and Methods

2.1. Cell Culture and Virus Infection

ECV304 cells were preserved and provided by the laboratory of the Department of Nephrology, Southern Hospital. Herpes simplex virus type II (HSV-2) strain was obtained from the General Hospital of Guangzhou Military Region of the Chinese People's Liberation Army. The HSV-2 strain was inoculated into Vero cells, and the virus was collected after 6 days and the titer was measured (50% tissue cell infection, TCID50 of $10^{5.5}$/mL). ECV304 cells were maintained in a maintenance medium (MEM, Gibco, US) supplemented with 10% fetal bovine serum, glutamine, sodium bicarbonate, penicillin, and streptomycin in a 37˚C, 5% CO_2 humidified incubator. Controls were added directly to the maintenance culture under the same conditions. Cultured cells and their controls were sampled at 2, 4 and 6 days after virus inoculation. Sample three times continuously within thirty minutes for subsequent experiments.

2.2. DNA Extraction and PCR

The LAT gene was amplified by PCR using the primer set: (forward: 5'-GTCAACACGGACACACTCTTTT-3') and (reverse: 5'-CGAGGCCTGTT-GGTCTTTATC-3'), which could be used to produce a 150-bp fragment. DNA was extracted from cells of the control group and infected groups at 12 h and 24 h post-infection using a DNA extraction kit for PCR detection of the HSV LAT gene. The total volume of the amplification reaction system was 50 μL, including 5 μL of DNA sample, 25 μL of 2 × Premix PCR premix buffer, 20 μmol/L of upstream and downstream primers of 1 μL each, and 18 μL of ddH_2O. Cycling conditions were as follows: pre-denaturation of 5 min at 94˚C, main cycle (1 min at 94˚C, 30 s at 65˚C, 1 min at 72˚C) for 30 cycles, and extension of 5 min at 72˚C. The amplification product was identified by 1.5% agarose gels (TaKaRa company, China).

2.3. Detection of HSV Infection by Indirect Immunofluorescence

HSV-2 pp65 protein expression was detected by immunofluorescence assay. ECV304 cell crawl sheets were prepared and inoculated with virus for 24 h. Infected and uninfected cells were fixed at room temperature with a fixed solution containing 2% paraformaldehyde and 0.1% Triton X-100 for 30 min, washed twice with PBS, blocked with normal goat serum for 20 min, and washed three times with PBS. Cell crawls were incubated with mouse anti-HSV-2 pp65 (US Biological, USA) for 30 min at 37˚C, and washed five times with PBS. The secondary antibody conjugated with FITC was subsequently added and incubated for 30 min at 37˚C, washed three times with PBS and observed under a fluorescence microscope (Nikon TE-2000, US).

2.4. Microarray Hybridization and Image Analysis

Total RNA was extracted using the Trizol extraction kit (Life Technologies INC.)

and the concentration and total amount of RNA was quantified by UV spectrophotometry at 260 and 280 nm. RNA samples with an A260/A280 ratio between 1.8 and 2.0 were selected. Total RNA from uninfected and infected ECV304 cells was reverse transcribed using the RNA Fluorescent Linear Amplification Kit (Agilent) and labeled with Cy5-dCTP and Cy3-dCTP, respectively. Cy5-labeled and Cy3-labeled targets were purified using Rneasy Mini Spin Columns (Qiagen) and then mixed and hybridized to Oligo Microarray Kit (Qiagen). The hybridization volume was 400 μL and consisted of 0.75 μg of each Cy3-labeled and Cy5-labeled linearly amplified cRNA, 50μL of 10 × control target and 225 μL of 2 × hybridization buffer. The mixture was vibrated and centrifuged, pipetted onto a cover glass, and covered with Agilent human 1B oligonucleotide chip. The hybridization box was hybridized at 60˚C and 4 rpm for 16 h, washed twice in 6 × SSC and 0.005% Triton X-102 solution at room temperature for 10 min each time, and then wash it in cold solution (0.1 × SSC, 0.005% Triton X-102) for 5 min. The slides were dried with nitrogen and stored in dark. The chip is scanned in the Agilent 2565BA gene chip scanner (Agilent, Palo Alto, CA, USA). The default parameters of the scanner are used for parameter setting. The scanned data are analyzed and homogenized by Feature extraction software. According to Cy3 (g processed signal) and Cy5 (r processed signal) Log ratio P-Value, $P < 0.01$ indicated a significant difference in gene expression between the virus-infected group and the control group. G processed signal < r processed signal was defined as up-regulation of gene expression, and g processed signal > r processed signal was defined as down-regulation of gene expression.

2.5. Validation of Microarray Results by Real-Time qPCR

Total RNA was extracted from ECV304 cells infected with HSV-2 and the control group for 6 h. Prepare the RT reaction solution (on ice) as per the reverse transcription kit. The reverse transcription was carried out under the following conditions: 10 min at 42˚C, and 2 min at 95˚C. The chip was verified by real-time qPCR, and a Rotor Gene 3000 Fluorescence quantitative detection system was detected by the SYBR RT-PCR kit. The genes to be tested and the sequence of GAPDH primers are shown in **Table 1**. The final volume of the 20 μL reaction mixture consisted of PCR mixture, diluted cDNA, and specific primers for two up-regulated genes and two down-regulated genes selected from the differentially expressed genes. The PCR reaction was carried out under the following conditions: an initial denaturation of 2 min at 95˚C; 30 cycles, each cycle consisting of 2 min at 95˚C, 94˚C, 1 min at 54˚C, and 1 min at 72˚C. At the end of the procedure, the specificity of the primer group was confirmed by the analysis of the neutrophilic curve. RT-PCR results were compared at different dilutions (10^0, 10^{-1}, 10^{-2}, 10^{-3}, 10^{-4}, 10^{-5} copies/reaction) to estimate the copy number of the target gene and GAPDH mRNA. Taking the housekeeping gene GAPDH as the internal standard (IS), the quantitative results of GAPDH in the HSV-infection Group and the Control Group were calculated through the standard curve of the housekeeping

gene, and the error of RNA quantity (relative quantity) was calculated. Each target gene was quantified by its standard curve, and the errors of the two groups of housekeeping genes were corrected. The corrected quantitative results of the target gene were compared to obtain the relative ratio of the two.

Table 1. Specific primers used in qRT-PCR analysis.

Gene name	Forward primer (5' - 3')	Downstream primers (5' - 3')
GAPDH	GCACCGTCA AGGCTGAGA AC	ATGGTGGTGAAGACGCCAGT
SP100	AAAGTTGAGTGCCAAGCCCAAG	TCTAAGGGCTCATCAACGTCAGTG
RPS24	GACAACTGGCTTTGGCATGATTTA	CCA ACA TTGGCCTTTGCAGTC
HNRPA1	AGGCTGGCAGATACG TTCGTC	CCTCAGGCTCTCATCAGTTGTTTC
RTP801	GCAGGACGCACTTGTCTTAGCA	CCA AAGGCTAGGCATGGTGAG

2.6. Statistical Processing

Statistical analysis was performed using SPSS10.0. One-Way ANOVA test was used to compare group means and differences between multiple groups. A P-value < 0.05 was considered significant.

3. Results

3.1. LAT Gene Testing

The HSV LAT gene is the first gene expressed after the virus invades the host cell. Since the presence of viral mRNA in the host cell is an important indicator of viral replication, the detection of viral LAT mRNA expression indicates active HSV infection. In the present study, PCR amplification of HSV-2 LAT gene after infection of cells with virus and viral supernatant was consistent with the expected results, indicating the possibility of direct virus infection to cells (**Figure 1**).

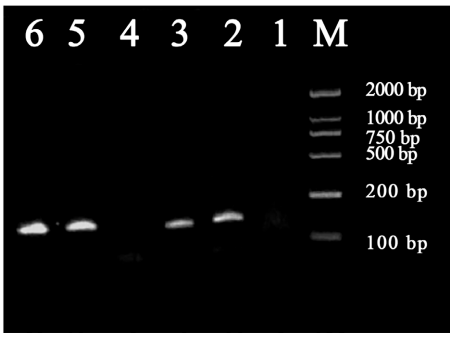

M: DNA Marker; 1, 4: Control; 2, 3: 12 h Post-infection; 5, 6: 24 h Post-infection.

Figure 1. Electrophoreosis of PCR products of HSV-2 LAT gene.

3.2. Detection of LAT Protein

Two days after viral infection, most cells showed a large fluorescent signal around

the nucleus (Figure 2(A)). The control group had a homogeneous cell background with no strong fluorescent signal (Figure 2(B)). This finding suggests that HSV-2 can infect ECV304 cells and proliferate in their cytoplasm.

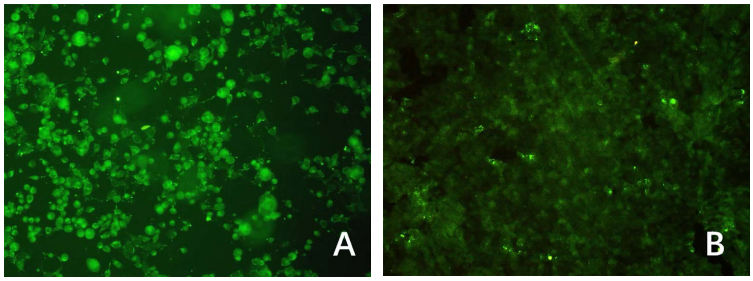

Figure 2. Immunofluorescence was used to detect the expression of the LAT gene in ECV304 cells 2 days after ECV304 infection (200×). (A) Control group; (B) ECV304 cells (green fluorescence showed positive LAT protein in infected cells).

3.3. Identifying the Quality of RNA

The RNA quantification results are as follows: The RNA of the control group is 1149 ng/μL, with an A260/A280 ratio of 1.8. The RNA of the HSV-2 infection group is also 1149 ng/μL, with an A260/A280 ratio of 1.81. The samples were subjected to agarose gel electrophoresis to identify the quality of RNA, and electrophoresis showed three clear RNA bands with visible 28S, 18S and 5S, and the samples were of high purity and integrity, in accordance with the DNA microarray requirements (Figure 3). Qualified samples were stored at −80˚C.

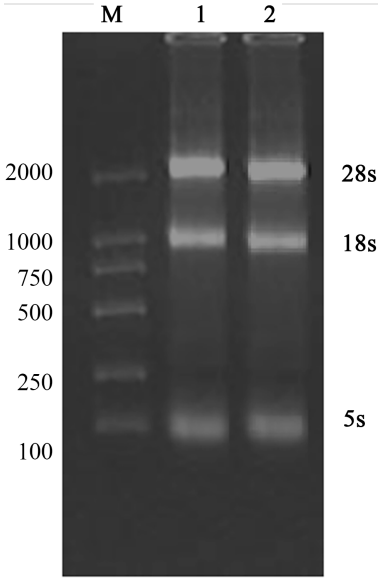

M: Marker; 1: Control; 2: HSV-2 infection.

Figure 3. Electrophoresis result of total RNA sample.

3.4. Quality Control of Microarray Hybridization

In the Agilent 2565BA gene microarray scanner, the microarrays were scanned

with the default parameters of the scanner, and the scanned data were analyzed and homogenized using the feature extraction software. The scanned results of the hybridized gene expression profiling microarrays were in accordance with the standard, with high signal intensity and uniform background (Figure 4).

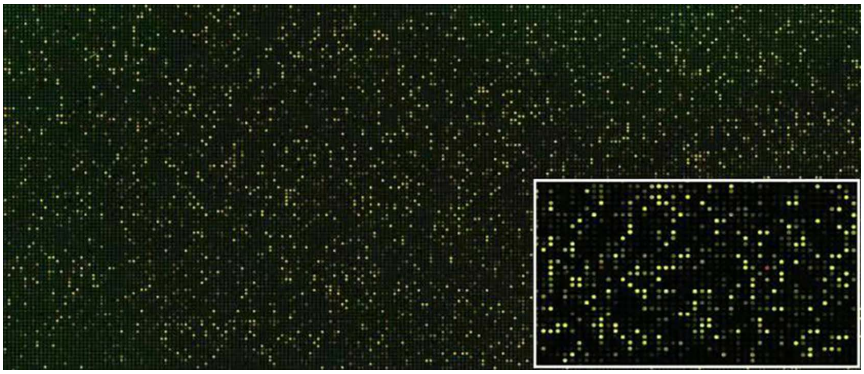

Figure 4. Microarray hybridization scanning picture.

3.5. Scatter Plots of Hybridizing Signal

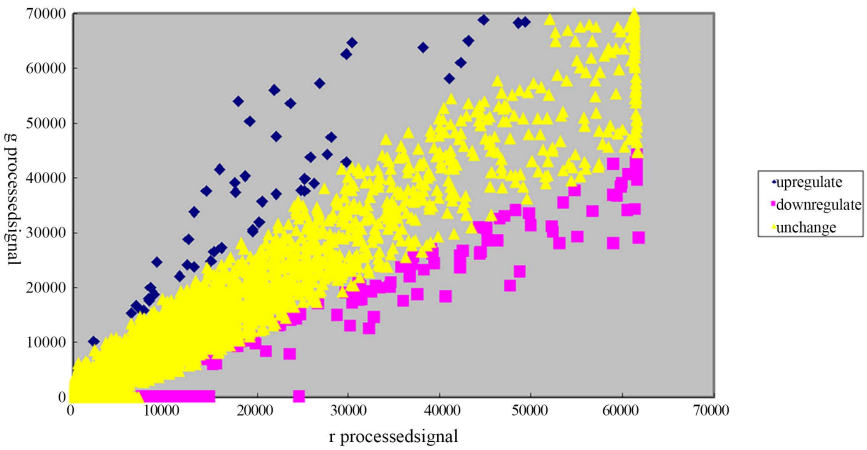

Figure 5. Scatter plot of Cy3/Cy5 hybridization intensity in the microarray. The fluorescence intensity of the chip was analyzed by scattergraph. Taking process signal (Cy3) as ordinate and process signal (Cy5) as abscissa, a scatter plot of fluorescence intensity of all points was drawn.

Gene Chip scatter plot analysis elucidates the intensity of fluorescent hybridization signals. As depicted in Figure 5, the horizontal axis represents Cy3 fluorescence intensity values, while the vertical axis represents Cy5 fluorescence intensity values. Each data point on this plot signifies the hybridization signal emanating from a specific gene locus on the microarray. The color of these data points conveys information about differential expression: yellow indicates no differential expression, whereas blue or red hues signify differential expression. The ECV-304 cells, subject to experimental (Cy3) and control (Cy5) conditions, exhibit a two-color fluorescent marker overlay. When these two fluorescent signals overlap at a single point, the resultant color provides insights into gene expression trends.

Specifically, a stronger Cy3 signal renders the point green, suggesting an up-regulation trend. Conversely, a stronger Cy5 signal results in a red point, indicating a down-regulation trend. When the intensities of both signals are comparable, the point appears yellow.

3.6. Differential Expressed Genes in HSV-2 Infected ECV304 Cells

When the fluorescence signal reaches a certain intensity, data points with ratios greater than 1.37 or less than 0.7 are selected. Data points with signal intensities greater than 5×10^8 were considered valid data points, and data points with ratios greater than 1.37 or less than 0.7 were considered to have significant expression changes. Based on the selection criteria, 17,575 valid data points were extracted from the microarray results, and a total of 462 differentially expressed genes were extracted. 318 genes were up-regulated (ratio more than 1.37); 144 genes were down-regulated (ratio less than 0.7) (Table 2). Positive values indicate up-regulation, while negative values describe down-regulation.

Table 2. Differential display of genes expressed in ECV 304 infected with HSV-2.

Gene Symbol	Ratio (g/r)	Gene Symbol	Ratio (g/r)	Gene Symbol	Ratio (g/r)
IL9	111.7176	PSMA7	4.3616	RPS5	3.1848
NAG-7	36.2037	RPS23	4.3444	HOXA3	3.1625
ATP6V0A2	30.6709	UQCRH	4.2248	PTMA	3.1382
I_1100038	8.7079	HSPC016	4.1982	VIM	3.0837
RPLP1	8.2655	RPL34	4.1579	RPL7A	3.0814
RPS10	7.8284	I_1000200	4.1499	LAMR1	3.0735
MT2A	7.4679	MT1E	4.0840	RPL7	3.0290
I_1109418	7.0383	RPL10A	4.0734	RPL13A	3.0256
FTH1	6.9516	ZFPM1	4.0569	APP	2.9978
RPS20	6.7500	RPL35	3.9349	RPS24	2.9796
RPL36A	6.6287	RPS11	3.9325	LU	2.9455
RPL19	6.4475	RPS14	3.9083	PABPC1	2.9446
RPL38	6.2619	RPS25	3.8745	IGFBP7	2.9329
RPL23A	6.1302	RPL8	3.8569	ANAPC11	2.8797
RPL26	6.0291	MT1B	3.8338	BTF3	2.8327
RPS27A	5.9390	UBC	3.7614	NSEP1	2.8307
RPS29	5.8372	RPS17	3.7474	RPL11	2.8280
S100A6	5.6553	EEF2	3.7165	RPS8	2.7911
RPS18	5.6445	MIF	3.6554	RPLP0	2.7563
RPL27	5.5780	NQO1	3.6068	I_962007	2.7405
EEF1B2	5.5078	OAZ1	3.5915	I_1847600.FL1	2.7162

Continued

RPL31	5.4858	MT1H	3.4805	I_958592	2.7154
RPL37A	5.4226	RPS15A	3.4709	GPX1	2.7026
SUI1	5.4220	RPL39	3.4672	MT1A	2.6876
RPL26	5.3642	LRRN1	3.4660	HIST1H4C	2.6689
I_1002391	5.3147	CALM2	3.4604	RPL30	2.6677
CAM-KIIN	5.3061	RPL24	3.4533	PTMS	2.6490
I_963838	5.2654	RPS28	3.4451	I_966336	2.6435
RPL12	5.2032	MAP3K10	3.4417	I_1109768	2.6310
RPL9	5.0539	RPS6	3.3936	KIAA0616	2.6284
LOC51142	5.0194	NME2	3.3849	NM_000983.2	2.6241
RPS21	5.0185	RPL41	3.3441	FLJ22184	2.6229
ATP5E	4.9273	NM_139020.1	3.3386	HES7	2.6205
RPS12	4.9041	TUBA6	3.3351	EIF3S3	2.6144
RPL37	4.8491	RPS16	3.3208	NM_178438.1	2.6101
C21orf6	4.7727	MT1K	3.3205	GAPD	2.6071
RPS27	4.7202	RPL27A	3.2840	GLTSCR2	2.6041
RPL35A	4.6320	I_963575	3.2436	MTCO2	2.6002
NM_006082.1	4.4970	RPL17	3.2110	VGF	2.5959
RPS13	4.4756	RPL23	3.1938	NM_178430.1	2.5736
RPS2	2.5501	HSPA5	2.1935	DTYMK	1.9531
PP2447	2.5492	EBNA1BP2	2.1859	TMSB10	1.9490
H2AFZ	2.5349	NM_178511.1	2.1853	COX6A1	1.9465
RPS15	2.5000	NM_000398.3	2.1832	I_1201840	1.9410
MT1J	2.4955	EEF1D	2.1763	S100A10	1.9405
RPS3A	2.4749	I_1000395	2.1550	TUBA1	1.9351
ID1	2.4594	MTND1	2.1545	PROL2	1.9144
GRIN2D	2.4444	NDUFC2	2.1482	MRPS24	1.8799
HCN2	2.4259	I_961758	2.1462	ATP5G3	1.8573
FAU	2.4240	MGC14353	2.1321	NM_003017.2	1.8535
HES1	2.4212	FBL	2.1311	H3F3B	1.8280
NDUFB2	2.4136	DUX4	2.1310	DIA1	1.8203
NM_001743.3	2.4102	NM_005251.1	2.1301	PRO0478	1.8193
PARD6G	2.3801	DKFZp434N0650	2.1238	LOC51219	1.8170
NDUFS5	2.3533	LSAMP	2.1204	GNG11	1.8153
RPL21	2.3337	RPL32	2.1155	EGR1	1.8146
CKS2	2.3328	COX7C	2.1142	HSPA1A	1.8122

Continued

SFRS9	2.3299	I_1152056	2.1133	NM_145293.1	1.8055
I_959447	2.3260	TPT1	2.1102	SSR2	1.8048
MT1X	2.3242	SNK	2.1065	H2AV	1.7792
DKFZp434N074	2.3097	MTND3	2.1002	LDHB	1.7750
FLJ14464	2.3068	SP100	2.0971	I_1000283	1.7707
STMN1	2.3054	ATP5O	2.0886	RPL14	1.7664
DBI	2.3020	COX7A2	2.0827	DAP	1.7645
HSPA8	2.2911	I_931617	2.0797	I_964413	1.7492
DRD4	2.2910	COX8	2.0775	FTL	1.7473
NM_152350.1	2.2761	SLC25A5	2.0500	CCT5	1.7348
HSPE1	2.2726	MT2A	2.0420	THOC4	1.7294
HINT1	2.2725	KRT18	2.0291	RoXaN	1.7275
EEF1A1	2.2678	NCL	2.0277	HMGB1	1.7216
CASKIN1	2.2615	ARF1	2.0275	DKFZp762E1312	1.7183
H2AFX	2.2557	CKLFSF3	2.0187	NOLA2	1.7032
POLR2L	2.2444	NNMT	2.0158	TXN	1.7009
GSTP1	2.2436	RAB34	2.0139	ATP5L	1.6978
LGALS1	2.2373	TK1	1.9980	I_1000105	1.6892
LBX1	2.2227	RPL4	1.9735	ZFP36L2	1.6889
VHL	2.2149	I_960618	1.9724	I_931932	1.6873
RPS4X	2.2147	HIST1H4L	1.9623	NM_003358.1	1.6863
CCT4	2.1969	SNRPG	1.9589	NXT1	1.6851
SEPW1	1.6782	NM_173609.1	1.5329	RBM8A	0.7166
TPSG1	1.6712	I_964798	1.5291	SNRPD1	0.7151
SLC25A3	1.6579	PCNA	1.5230	WBSCR1	0.7001
FLJ20308	1.6578	PCBP1	1.5212	APPBP1	0.6981
POLR2A	1.6538	CMT2	1.5142	PSMB6	0.6954
HNRPM	1.6532	YWHAB	1.5060	PYCR1	0.6948
RPL10	1.6495	TNFRSF1A	1.5048	HSPCB	0.6936
PLP2	1.6392	NDUFB4	1.5034	ANXA2	0.6895
TEBP	1.6368	EIF3S9	1.4982	DNAJC9	0.6855
NM_003769.1	1.6275	C20orf24	1.4963	CCT3	0.6848
MT1H	1.6255	MRPS12	1.4917	GARS	0.6845
UNRIP	1.6048	NM_022833.1	1.4869	PDHA1	0.6839
RPL36AL	1.6005	SERF2	1.4865	NDUFS6	0.6838
OCSP	1.5976	SLC21A12	1.4849	SF3B1	0.6758

Continued

QP-C	1.5974	I_957363	1.4813	I_1110347	0.6753
I_932488	1.5964	LOC51685	1.4707	I_1109809	0.6738
UBL1	1.5957	NACA	1.4686	MCM3	0.6704
U2AF1	1.5939	DNCL1	1.4640	ITGAM	0.6673
TGFA	1.5907	MORF4L2	1.4540	MTHFD2	0.6672
SEC61B	1.5839	I_951081	1.4475	FLJ11323	0.6591
RPL15	1.5826	LAMP1	1.4449	LMNA	0.6591
HIST2H2AA	1.5816	BLCAP	1.4415	HSPA9B	0.6588
SF1	1.5815	UQCR	1.4393	MGC4308	0.6568
NME1	1.5814	NM_178352.1	1.4379	PPIA	0.6507
CDC42	1.5759	AKAP2	1.4374	NEUGRIN	0.6498
MGC10974	1.5756	RPL5	1.4328	PSA	0.6488
SFPQ	1.5729	MGAT1	1.4283	NASP	0.6393
FHL2	1.5616	PSME2	1.4211	CD59	0.6383
NDUFS3	1.5587	HIST3H3	1.4201	FLJ23209	0.6341
RPS3	1.5585	I_1152035	1.4183	RRM1	0.6339
HIS1	1.5579	NM_138425.1	1.4156	PSMC1	0.6310
EEF1G	1.5558	I_1000097	1.4115	RARS	0.6260
PC4	1.5514	PTTG1	1.4052	GSTTLp28	0.6246
NEDD8	1.5479	PABPC3	1.4025	SFRS7	0.6226
PCBP2	1.5460	I_932347	1.3941	DKFZp566H0824	0.6220
PSMB1	1.5439	CCT2	1.3919	RHO	0.6208
SOD1	1.5437	LENG5	1.3876	SNRPA1	0.6155
I_930805	1.5384	EIF2S2	1.3812	STMN4	0.6154
ZFP36L1	1.5363	CBS	1.3766		
LOC147700	0.6118	PFDN2	0.5141	YEA	0.0009
I_960911	0.6109	EIF3S2	0.5094	BAIAP1	0.0008
PCK2	0.6105	I_960077	0.4929	HSD3B7	0.0008
PAICS	0.6084	DDB1	0.4832	ALDOC	0.0008
HNRPDL	0.6054	I_1000514	0.4793	I_964921.FL2	0.0008
FLJ90165	0.6008	I_1110080	0.4735	I_1000255	0.0008
UBCE7IP5	0.5999	EIF4A1	0.4678	GML	0.0008
I_931957	0.5981	I_1000329	0.4639	WBP4	0.0008
MRPL22	0.5980	HUMAUANTIG	0.4554	DNASE2	0.0008
I_1000009	0.5951	ANXA1	0.4480	PPIL4	0.0008
GP2	0.5926	ACTB	0.4374	NEU4	0.0008

Continued

RBM3	0.5903	TPM1	0.4280	TRNT1	0.0008
I_1151867	0.5899	C20orf97	0.4213	MTERF	0.0008
PSMB7	0.5887	CLIC1	0.3868	MFNG	0.0007
CEBPB	0.5884	NM_173624.1	0.3830	MGC21738	0.0007
I_928538	0.5884	HSPCA	0.3799	GGCX	0.0007
I_965066	0.5844	HNRPA1	0.3795	ZNF333	0.0007
I_1109622	0.5842	RTP801	0.3263	FLJ20333	0.0007
FLJ20700	0.5794	CELSR1	0.0017	ZNF215	0.0007
ARHGEF15	0.5783	FLJ20695	0.0014	CACH-1	0.0007
FLJ10097	0.5759	SORCS3	0.0013	G22P1	0.0007
FLJ21174	0.5743	SPP1	0.0012	ACAS2L	0.0007
CENPF	0.5694	PIGO	0.0011	FUT5	0.0007
I_962171	0.5617	I_1110369	0.0011	I_1000094	0.0006
SSRP1	0.5593	PROSC	0.0011	LOC51185	0.0006
I_962014	0.5588	I_961649	0.0010	NM_144963.1	0.0006
RPL6	0.5583	eQC	0.0010	BRUNOL6	0.0006
IL30	0.5571	MCCC2	0.0010	NM_138350.1	0.0006
I_965611	0.5539	I_966078	0.0009	C22orf2	0.0006
HEC	0.5538	I_963210	0.0009	ZNF267	0.0006
THOC3	0.5445	I_934625	0.0009	PIG3	0.0005
NM_006088.2	0.5425	DBR1	0.0009	SPP1	0.0005
RA410	0.5376	SCGB1A1	0.0009	NM_145300.1	0.0005
HMGN2	0.5271	MLANA	0.0009	I_931899	0.0003
DNAJA1	0.5266	ANKRA2	0.0009		
CYCS	0.5248	NM_173501.1	0.0009		

3.7. Verification of Gene Chip Results

Table 3. Relative quantitation results of real time RT-PCR.

		IS (GAPDH)		Target Gene		Relative
		Quantitative Results (copies)	Relative (X)	Quantitative Results (Y) (copies)	Quantitative results after correction (Y/X)	
SP100 gene	Control	12,698,991	1	8,212,159	8212159.0	1
	Infect	6,223,228	0.490	8,800,188	17957484.0	2.187
RPS24 gene	Control	12,698,991	1	12,835,309	12835309.0	1
	Infect	6,223,228	0.490	10,901,163	22244690.7	1.733
RTP801 gene	Control	12,698,991	1	479358511	479358511.0	1
	Infect	6,223,228	0.490	49557264	101125541.9	0.211
HNRPA1 gene	Control	12,698,991	1	30478756	30478756.0	1
	Infect	6,223,228	0.490	24397428	49784894.2	1.633

Table 4. Compared the Results of Real Time RT-PCR and Microarray.

	Real Time RT-PCR Quantitative Results	Gene chip test results
SP100 gene	2.187	2.097
RPS24 gene	1.733	2.980
RTP801 gene	0.211	0.326
HNRPA1 gene	1.633	0.380

Four genes were selected and validated by real-time quantitative PCR using double-stranded DNA combined with SYBR Green I. The quantitative results were generally consistent with the gene microarray detection results, which illustrated the reliability of the human whole-genome oligonucleotide expression profiling microarray in screening differentially expressed genes (**Table 3** & **Table 4**).

3.8. Analysis of Differential Genes Involved in Biological Processes

The differential genes were uploaded to the Internet bioinformatics analysis professional website to analyze the biological processes involved in the differential genes (https://panther.appliedbiosystems.com/), and it was found that 462 differential genes were involved in a total of 237 biological processes, 79 of which were significantly different ($P < 0.05$), as shown in **Table 5**. The results showed that 73 genes related to protein synthesis, such as *RPS*, *RPL*, *EEF* and *SUI1*, were generally up-regulated 6 h after HSV-2 infection of ECV304 cells. *HSPA8*, *HSPE1*, *CCT2*, *CCT4* and *CCT5* genes related to protein elongation and folding were up-regulated, and 9 genes such as *HSPCB*, *HSPCA*, *CCT3* and *PPIA* were down-regulated; 12 genes related to cell signaling such as *CASK*, *APP* and *HINT1* were up-regulated, and 5 genes such as *RHO* and *CELSR1* were down-regulated.

Table 5. Analysis of gene expression profiles in ECV 304 infected with HSV-2.

№	Biological process	Unigene ID	Entrez Gene	Symbol	chip Ratio
1	protein biosynthesis	356502	6176	RPLP1	8.2655
		406620	6204	RPS10	7.8284
		8102	6224	RPS20	6.7500
		432485	6173	RPL36A	6.6287
		381061	6143	RPL19	6.4475
		380953	6169	RPL38	6.2619
		419463	6147	RPL23A	6.1302
		482144	6154	RPL26	6.0291
		311640	6233	RPS27A	5.9390
		156367	6235	RPS29	5.8372
		546290	6222	RPS18	5.6445
		514196	6155	RPL27	5.5780

Continued

		421608	1933	EEF1B2	5.5078
		523670	6160	RPL31	5.4858
		433701	6168	RPL37A	5.4226
		150580	10209	SUI1	5.4220
		408054	6136	RPL12	5.2032
		412370	6133	RPL9	5.0539
		190968	6227	RPS21	5.0185
		546289	6206	RPS12	4.9041
		80545	6167	RPL37	4.8491
		546291	6232	RPS27	4.7202
		182825	11224	RPL35	4.6320
		529631	6165	RPL35A	4.6320
		446588	6207	RPS13	4.4756
		386384	6228	RPS23	4.3444
		438227	6164	RPL34	4.1579
		148340	4736	RPL10A	4.0734
		433529	6205	RPS11	3.9325
		381126	6208	RPS14	3.9083
1	protein biosynthesis	178551	6132	RPL8	3.8569
		433427	6218	RPS17	3.7474
		515070	1938	EEF2	3.7165
		370504	6210	RPS15A	3.4709
		546284	6170	RPL39	3.4672
		547172	6152	RPL24	3.4533
		153177	6234	RPS28	3.4451
		408073	6194	RPS6	3.3936
		381172	6171	RPL41	3.3441
		397609	6217	RPS16	3.3208
		523463	6157	RPL27A	3.2840
		374588	6139	RPL17	3.2110
		406300	9349	RPL23	3.1938
		378103	6193	RPS5	3.1848
		499839	6130	RPL7A	3.0814
		421257	6129	RPL7	3.0290
		546356	23521	RPL13A	3.0256
		356794	6229	RPS24	2.9796
		388664	6135	RPL11	2.8280

Continued

		546285	6175	RPLP0	2.7563
		400295	6156	RPL30	2.6677
		492599	8667	EIF3S3	2.6144
		356366	6187	RPS2	2.5501
		406683	6209	RPS15	2.5000
		356572	6189	RPS3A	2.4749
		387208	2197	FAU	2.4240
		381123	6144	RPL21	2.3337
		520703	1915	EEF1A1	2.2678
		446628	6191	RPS4X	2.2147
		333388	1936	EEF1D	2.1763
		265174	6161	RPL32	2.1155
		186350	6124	RPL4	1.9735
		446522	9045	RPL14	1.7664
		401929	6134	RPL10	1.6495
1	protein biosynthesis	444749	6166	RPL36AL	1.6005
		381219	6138	RPL15	1.5826
		546286	6188	RPS3	1.5585
		144835	1937	EEF1G	1.5558
		371001	8662	EIF3S9	1.4982
		411125	6183	MRPS12	1.4917
		505735	4666	NACA	1.4686
		532359	6125	RPL5	1.4328
		429180	8894	EIF2S2	1.3812
		520943	7458	WBSCR1	0.7001
		404321	2617	GARS	0.6845
		506215	5917	RARS	0.6260
		483924	29093	MRPL22	0.5980
		546283	6128	RPL6	0.5583
		530096	8668	EIF3S2	0.5094
		129673	1973	EIF4A1	0.4678
		546291	6232	RPS27	4.7202
		466743	4294	MAP3K10	3.4417
		434980	351	APP	2.9978
2	signal transduction	155048	4059	LU	2.9455
		445015	2906	GRIN2D	2.4444
		99922	1815	DRD4	2.2910

Continued

		483305	3094	HINT1	2.2725
		530863	57524	CASKIN1	2.2615
		83381	2791	GNG11	1.8153
		435136	7295	TXN	1.7009
		50425	10728	TEBP	1.6368
2	signal transduction	279594	7132	TNFRSF1A	1.5048
		460978	8883	APPBP1	0.6981
		247565	6010	RHO	0.6208
		523560	3320	HSPCA	0.3799
		252387	9620	CELSR1	0.0017
		523732	7356	SCGB1A1	0.0009
		180414	3312	HSPA8	2.2911
		1197	3336	HSPE1	2.2726
		421509	10575	CCT4	2.1969
		520028	3303	HSPA1A	1.8122
		1600	22948	CCT5	1.7348
		534385	10189	THOC4	1.7294
		50425	10728	TEBP	1.6368
		189772	10576	CCT2	1.3919
3	protein folding	509736	3326	HSPCB	0.6936
		523037	23234	DNAJC9	0.6855
		491494	7203	CCT3	0.6848
		184233	3313	HSPA9B	0.6588
		356331	5478	PPIA	0.6507
		445203	3301	DNAJA1	0.5266
		492516	5202	PFDN2	0.5141
		523560	3320	HSPCA	0.3799
		551568	85313	PPIL4	0.0008
		180414	3312	HSPA8	2.2911
		1197	3336	HSPE1	2.2726
4	response to unfolded protein	520028	3303	HSPA1A	1.8122
		509736	3326	HSPCB	0.6936
		445203	3301	DNAJA1	0.5266
		523560	3320	HSPCA	0.3799
5	positive regulation of nitric oxide biosynthesis	509736	3326	HSPCB	0.6936
		523560	3320	HSPCA	0.3799
6	protein refolding	523560	3320	HSPCA	0.3799

Continued

		516076	6637	SNRPG	1.9589
		365116	7307	U2AF1	1.5939
7	RNA splicing	355934	6421	SFPQ	1.5729
		309090	6432	SFRS7	0.6226
		528763	6627	SNRPA1	0.6155
		369624	8683	SFRS9	2.3299
		79110	4691	NCL	2.0277
		534385	10189	THOC4	1.7294
		365116	7307	U2AF1	1.5939
		355934	6421	SFPQ	1.5729
		552581	9939	RBM8A	0.7166
		464734	6632	SNRPD1	0.7151
8	nuclear mRNA splicing	471011	23451	SF3B1	0.6758
		309090	6432	SFRS7	0.6226
		527105	9987	HNRPDL	0.6054
		484227	84321	THOC3	0.5445
		546261	3178	HNRPA1	0.3795
		411300	11193	WBP4	0.0008
		348342	60677	BRUNOL6	0.0006
		534385	10189	THOC4	1.7294
		552581	9939	RBM8A	0.7166
9	mRNA-nucleus export	484227	84321	THOC3	0.5445
		546261	3178	HNRPA1	0.3795
		546271	5094	PCBP2	1.5460
10	mRNA metabolism	2853	5093	PCBP1	1.5212
		458280	5042	PABPC3	1.4025
11	mRNA stabilization	387804	26986	PABPC1	2.9446
12	RNA transcription termination	532216	7978	MTERF	0.0008
13	tRNA 3'-processing	506382	51095	TRNT1	0.0008
14	glycyl-tRNA aminoacylation	404321	2617	GARS	0.6845
15	arginyl-tRNA aminoacylation	506215	5917	RARS	0.6260
		150580	10209	SUI1	5.4220
16	translational initiation	371001	8662	EIF3S9	1.4982
		429180	8894	EIF2S2	1.3812
		150580	10209	SUI1	5.4220
		492599	8667	EIF3S3	2.6144
17	regulation of translational initiation	520943	7458	WBSCR1	0.7001
		530096	8668	EIF3S2	0.5094

Continued

18	regulation of translation	150580	10209	SUI1	5.4220
		520703	1915	EEF1A1	2.2678
		356502	6176	RPLP1	8.2655
		421608	1933	EEF1B2	5.5078
19	translational elongation	546285	6175	RPLP0	2.7563
		520703	1915	EEF1A1	2.2678
		333388	1936	EEF1D	2.1763
		144835	1937	EEF1G	1.5558
20	embryo implantation	523732	7356	SCGB1A1	0.0009
21	cytoplasmic sequestering of NF-kappaB	31210	602	BCL3	2.1500
22	iron ion transport	446345	2495	FTH1	6.9516
		517666	1727	DIA1	1.8203
		433670	2512	FTL	1.7473
23	ATP synthesis coupled proton transport	546238	514	ATP5E	4.9273
		409140	539	ATP5O	2.0886
		429	518	ATP5G3	1.8573
		486360	10632	ATP5L	1.6978
		201939	23545	ATP6V0A2	30.6709
24	proton transport	546238	514	ATP5E	4.9273
		409140	539	ATP5O	2.0886
		429	518	ATP5G3	1.8573
		486360	10632	ATP5L	1.6978
25	mitochondrial electron transport	324250	4708	NDUFB2	2.4136
		472185	4725	NDUFS5	2.3533
		407860	4718	NDUFC2	2.1482
		502528	4722	NDUFS3	1.5587
		304613	4710	NDUFB4	1.5034
		408257	4726	NDUFS6	0.6838
26	mitochondrial electron transport	481571	7388	UQCRH	4.2248
27	ribosomal protein-nucleus import	406300	9349	RPL23	3.1938
28	cysteine biosynthesis from serine	533013	875	CBS	1.3766
29	bile acid biosynthesis	460618	80270	HSD3B7	0.0008
30	DNA metabolism	471873	1841	DTYMK	1.9531
		350966	9232	PTTG1	1.4052
		118243	1777	DNASE2	0.0008
31	DNA replication and chromosome cycle	350966	9232	PTTG1	1.4052
		497741	1063	CENPF	0.5694

Continued

32	base-excision repair, DNA ligation	434102	3146	HMGB1	1.7216
33	regulation of DNA replication	147433	5111	PCNA	1.5230
34	DNA damage response	86161	2765	GML	0.0008
35	dTTP biosynthesis	471873	1841	DTYMK	1.9531
36	nucleotide metabolism	463456	4831	NME2	3.3849
		118638	4830	NME1	1.5814
		522099	84720	PIGO	0.0011
37	CTP biosynthesis	463456	4831	NME2	3.3849
		118638	4830	NME1	1.5814
38	UTP biosynthesis	463456	4831	NME2	3.3849
		118638	4830	NME1	1.5814
39	GTP biosynthesis	463456	4831	NME2	3.3849
		118638	4830	NME1	1.5814
40	nucleoside triphosphate biosynthesis	463456	4831	NME2	3.3849
		118638	4830	NME1	1.5814
41	dTDP biosynthesis	471873	1841	DTYMK	1.9531
42	purine base biosynthesis	518774	10606	PAICS	0.6084
43	polyamine biosynthesis	446427	4946	OAZ1	3.5915
44	aminoglycan biosynthesis	519818	4245	MGAT1	1.4283
45	prostaglandin biosynthesis	407995	4282	MIF	3.6554
		50425	10728	TEBP	1.6368
46	“de novo” IMP biosynthesis	518774	10606	PAICS	0.6084
47	cysteine biosynthesis via cystathione	533013	875	CBS	1.3766
48	anaerobic glycolysis	446149	3945	LDHB	1.7750
49	intracellular sequestering of iron ion	446345	2495	FTH1	6.9516
50	immune cell chemotaxis	313	6696	SPP1	0.0012
51	T-helper 1 type immune response	313	6696	SPP1	0.0012
52	regulation of myeloid cell differentiation	313	6696	SPP1	0.0012
53	negative regulation of bone mineralization	313	6696	SPP1	0.0012
54	induction of positive chemotaxis	313	6696	SPP1	0.0012
55	intracellular signaling cascade	209983	3925	STMN1	2.3054
		201058	81551	STMN4	0.6154
56	G-protein coupled receptor protein signaling pathway	99922	1815	DRD4	2.2910
		83381	2791	GNG11	1.8153
		247565	6010	RHO	0.6208
57	sensory perception	298198	123920	CKLFSF3	2.0187
		247565	6010	RHO	0.6208

Continued

58	rhodopsin mediated signaling	247565	6010	RHO	0.6208
59	phototransduction, visible light	247565	6010	RHO	0.6208
60	phosphoinositide-mediated signaling	83758	1164	CKS2	2.3328
		147433	5111	PCNA	1.5230
61	cellular morphogenesis	421597	7428	VHL	2.2149
62	positive regulation of cell differentiation	421597	7428	VHL	2.2149
		421597	7428	VHL	2.2149
63	proteolysis and peptidolysis	567440	25823	TPSG1	1.6712
		531064	4738	NEDD8	1.5479
64	cellular respiration	437060	54205	CYCS	0.5248
65	caspase activation via cytochrome c	437060	54205	CYCS	0.5248
66	acetyl-CoA metabolism	530331	5160	PDHA1	0.6839
67	peptidyl-glutamic acid carboxylation	77719	2677	GGCX	0.0007
68	spliceosome assembly	516076	6637	SNRPG	1.9589
		502829	7536	SF1	1.5815
69	ribosome biogenesis and assembly	499839	6130	RPL7A	3.0814
		546285	6175	RPLP0	2.7563
		27222	55651	NOLA2	1.7032
70	regulation of macrophage activation	407995	4282	MIF	3.6554
71	regulation of viral genome replication	356331	5478	PPIA	0.6507
72	positive regulation of fibroblast proliferation	275243	6277	S100A6	5.6553
73	positive regulation of translation	387804	26986	PABPC1	2.9446
74	negative regulation of transcriptional preinitiation complex formation	434102	3146	HMGB1	1.7216
75	negative regulation of cyclin dependent protein kinase activity	15299	10614	HIS1	1.5579
76	leucine catabolism	167531	64087	MCCC2	0.0010
77	nascent polypeptide association	505735	4666	NACA	1.4686
78	oxidative phosphorylation	481571	7388	UQCRH	4.2248
79	copper ion homeostasis	418241	4502	MT2A	7.4679
		434980	351	APP	2.9978

4. Discussion

Our investigation revealed that HSV-2 is capable of infecting ECV 304 cells, leading to a cascade of modifications in gene expression. These modifications encompass variations in the expression of genes associated with cell signaling, cytoskeletal dynamics and motility, cell cycle regulation, transcription and transcription factors, protein synthesis, ion channel activity, cellular receptors, immune responses, and metabolic processes.

Gene microarrays can monitor the expression levels of thousands of genes simultaneously on a large scale to study the relationship between abundant gene expression and disease. Gene microarray technology can be used to analyze the differential expression of genes during viral infection of host cells, which is important for the treatment of diseases [12].

Previous research showed that ECV304 cells were infected with HSV-2 and morphological changes of the cells were observed by contrast microscopy and tissue staining. It was found that cell necrosis was the predominant form of cell death, and no significant apoptosis was observed. Later, Zhang *et al*. [13] confirmed that HSV-2 infection of ECV304 cells significantly induced apoptosis. However, the relatively simple information obtained in the single-gene model makes it more difficult to perform a comprehensive in-depth analysis. Mo *et al*. [14] analyzed the effect of rubella virus (RUBV), human cytomegalovirus (HCMV), and HSV-2 co-infection on mRNA accumulation in ECV304 cells by using microarray technology, and found that 80 genes were up-regulated and 19 genes were down-regulated, including *VEGF*, *WISP2*, *WISP2* and *COL11A2*, etc. However, the effect of HSV-2 infection on the mRNA expression of ECV304 cells has not been studied by gene chip technology.

In this study, we used the ECV304 endothelial cell line as a model and human genome-wide oligonucleotide microarray to investigate the inhibitory effect of HSV-2 on ECV304 cells and to elucidate the expression of related genes. HSV-2 may play a role in signal transduction and regulation of gene expression in this process. The results showed that a total of 462 genes were significantly differentially expressed in the experimental group compared with the control group, of which 318 genes were up-regulated and 144 genes were down-regulated. The results showed that differential genes were involved in 237 biological processes, 79 of which were significantly different ($P < 0.05$).

These genes include cell signaling-related genes, cytoskeleton and motility-related genes, cell cycle-related genes, protein synthesis-related genes, transcription and transcription factor-related genes, and cell receptor-related genes. The results of the four differentially expressed genes validated by RT-PCR were generally consistent with those of the differentially expressed genes analyzed by gene microarray, indicating the reliability of the gene microarray data. Several genes that may be involved in endothelial damage and atherosclerosis caused by HSV-2 infection, which were identified for the first time in this study, are discussed below.

Heat shock proteins (HSP) are a family of proteins with important physiological functions that are highly conserved in evolution [15]. HSP can be classified into several families such as HSP110, HSP90, HSP70, HSP60, small molecule HSP and ubiquitin according to their molecular weight and degree of homology [16] [17]. Under adverse conditions such as stress, HSP can induce cell production, improve cell resistance, and play a role in stress protection, so it is also known as stress protein (SP). The main physiological functions of HSP are to promote and maintain the correct folding of new polypeptide chains [18], to participate in cell

damage and repair [19], and to regulate cell growth, division, differentiation and death [20] [21]. Our results show that HSV-2 also induces HSP production in ECV304 cells after infection, suggesting that upregulation of HSP may be involved in some HSV-2-mediated cell biological damage.

The ribosome is an important organelle in the cell responsible for protein synthesis and consists of four rRNAs and 80 ribosomal proteins (RP) [22] [23]. RP is an important component of the ribosome and plays an important role in the translation process of the ribosome, such as folding of rRNA to form a functional three-dimensional structure; adjusting the spatial conformation of the ribosome during protein synthesis; and catalyzing protein synthesis in concert with rRNA at the binding site of the ribosome. In our study, the expression of 36 *RPL* genes and 23 *RPS* genes related to protein synthesis was elevated, and only the expression of *RPL6* gene was decreased, indicating that the ribosomal protein gene is extensively involved in virus-cell interaction during the early stages of HSV-2 infection of ECV304 cells.

The S100 family of proteins is a group of EF-chiral calcium-binding proteins that play a variety of biological roles in vivo through regulation of calcium ions and interaction with target proteins, participating in cell cycle activities, cell differentiation, tumor growth, and extracellular matrix secretory activities [24]. Its distribution is cell- and tissue-specific [25], and several S100 members are abnormally expressed in tumors and are closely associated with tumor infiltration and metastasis. S100A6 is called calcyclin and used to be also known as 2A9, 5B10, and PRA. Chromosome 1q21 has been found to be altered in certain cancers or precancerous lesions, such as breast cancer, lymphoma and leukemia. From the specific expression of the biological function of the S100 protein family in tumors and its chromosomal localization, it can be found that it is closely related to tumors, of which S100A6 has increased expression in most tumor tissues. The results of this study showed that HSV-2 infection of ECV304 cells induced a 5.6-fold increase in cellular S100A6 gene expression. Combined with the results of many studies at home and abroad, which also showed that the development of cervical cancer may be related to HSV-2 infection, it suggests that the S100A6 gene may play some role in the development of cervical cancer. The aberrant expression of S100A6 is intricately associated with cellular proliferation and differentiation processes. Upon stimulation of quiescent cells by serum, epidermal growth factor, platelet-derived growth factor, nerve growth factor, retinoic acid, ischemic injury, and other physiological or pathological stimuli, there is a marked increase in the intracellular levels of S100A6 [26]. Existing literature indicates that S100A6 is significantly overexpressed in a variety of proliferative cell types, including ras-transformed NIH3T3 cells, SV40-transformed mouse fibroblasts, and various human malignancies such as acute myeloid leukemia, endometrial cancer, breast cancer, lung cancer, colorectal tumors, thyroid tumors, malignant fibrous histiocytoma, melanoma, neuroblastoma, squamous cell carcinoma of the oral mucosa, as well as in diverse epithelial-derived tumor cell lines. These cells exhibit elevated S100A6

expression levels in comparison to their differentiated or growth-inhibited counterparts [27].

Osteopontin (OPN) is a secreted acidic glycoprotein with multiple functions, classified as extracellular matrix, which promotes cell adhesion and migration [28]. OPN is present in human blood, urine, breast milk and other body fluids, as well as in the gastrointestinal tract, bladder, pancreas, lungs, bronchi and other tissues [29]. In our study, the expression of the *Spp1* gene was significantly reduced, which may be associated with HSV-2 infection, suggesting that the *Spp1* gene may play some role in the process of HSV-2 infection.

Calcium/calmodulin-dependent serine protein kinase (CASK) is a family of membrane-associated guanylate kinases. It was first cloned in nematodes [30], and its homologs were subsequently found in Drosophila and mammals [31]. CASK has several distinct protein binding domains and binds to other proteins to form protein complexes involved in the construction of the cell membrane protein backbone, cell signaling, gene regulation and many other important cellular physiological processes [32]. Current research on CASK is focused on the brain nervous system [33] and embryonic development [34]. With the accumulation of research data and advances in proteomics technology, it has become possible to understand the molecular network of various proteins that CASK interacts with in different cells and their related functions. Meanwhile, the establishment of knockout models of this protein in mammals will help to understand the role of CASK in overall biological development as well as in related diseases.

5. Conclusion

Among all biological processes induced by HSV-2 infection of ECV304 cells, 462 differential genes were found to be involved in a total of 237 biological processes, 79 of which were significantly different ($P < 0.05$). These mainly included biological processes such as protein synthesis, signaling, protein folding, RNA splicing, ion channels, ribosome synthesis and assembly, cellular respiration, DNA and mRNA metabolism. Further analysis revealed that a variety of genes among these differentially expressed genes may be involved in HSV-causing endothelial damage, cervical cancer and atherosclerosis, while the role of most other differentially expressed genes identified for the first time in the pathogenesis of HSV is unclear. Nevertheless, screening for aberrantly expressed genes by gene microarray provides valuable clues for an in-depth study of the mechanisms by which HSV causes endothelial injury and atherosclerosis.

Acknowledgements

We are grateful to Changwen Ke, director of the Institute of Microbiology Laboratory, Guangdong Center for Disease Control, for providing a high-quality laboratory and excellent instruments and equipment for the study of this topic, as well as giving valuable suggestions and enthusiastic guidance.

Funding

This work is supported by grants from the National Natural Science Foundation of China (No.31760716; 31560681), and the Project of Jiangxi Province (No. 20151BBF60007; 20171ACB21028).

Conflicts of Interest

The authors declare no conflicts of interest regarding the publication of this paper.

References

[1] Huang, Y., Song, Y., Li, J., Lv, C., Chen, Z. and Liu, Z. (2022) Receptors and Ligands for Herpes Simplex Viruses: Novel Insights for Drug Targeting. *Drug Discovery Today*, **27**, 185-195. https://doi.org/10.1016/j.drudis.2021.10.004

[2] Rechenchoski, D.Z., Faccin-Galhardi, L.C., Linhares, R.E.C. and Nozawa, C. (2016) Herpesvirus: An Underestimated Virus. *Folia Microbiologica*, **62**, 151-156. https://doi.org/10.1007/s12223-016-0482-7

[3] Tognarelli, E.I., Palomino, T.F., Corrales, N., Bueno, S.M., Kalergis, A.M. and González, P.A. (2019) Herpes Simplex Virus Evasion of Early Host Antiviral Responses. *Frontiers in Cellular and Infection Microbiology*, **9**, Article 127. https://doi.org/10.3389/fcimb.2019.00127

[4] Hechter, R.C., Budoff, M., Hodis, H.N., Rinaldo, C.R., Jenkins, F.J., Jacobson, L.P., *et al*. (2012) Herpes Simplex Virus Type 2 (HSV-2) as a Coronary Atherosclerosis Risk Factor in HIV-Infected Men: Multicenter AIDS Cohort Study. *Atherosclerosis*, **223**, 433-436. https://doi.org/10.1016/j.atherosclerosis.2012.03.002

[5] Wu, Y.P., Sun, D.D., Wang, Y., Liu, W. and Yang, J. (2016) Herpes Simplex Virus Type 1 and Type 2 Infection Increases Atherosclerosis Risk: Evidence Based on a Meta-Analysis. *BioMed Research International*, **2016**, 1-9. https://doi.org/10.1155/2016/2630865

[6] Kouyoumjian, S.P., Heijnen, M., Chaabna, K., Mumtaz, G.R., Omori, R., Vickerman, P., *et al*. (2018) Global Population-Level Association between Herpes Simplex Virus 2 Prevalence and HIV Prevalence. *AIDS*, **32**, 1343-1352. https://doi.org/10.1097/qad.0000000000001828

[7] Shi, Y. and Tokunaga, O. (2002) Herpesvirus (HSV-1, EBV and CMV) Infections in Atherosclerotic Compared with Non-Atherosclerotic Aortic Tissue. *Pathology International*, **52**, 31-39. https://doi.org/10.1046/j.1440-1827.2002.01312.x

[8] Ye, J., Li, J. and Zhao, P. (2021) Roles of ncRNAs as ceRNAs in Gastric Cancer. *Genes*, **12**, Article 1036. https://doi.org/10.3390/genes12071036

[9] Nunes, I.J.G., Recamonde-Mendoza, M. and Feltes, B.C. (2022) Gene Expression Analysis Platform (GEAP): A Highly Customizable, Fast, Versatile and Ready-to-Use Microarray Analysis Platform. *Genetics and Molecular Biology*, **45**, e20210077. https://doi.org/10.1590/1678-4685-gmb-2021-0077

[10] Mo, X., Ma, W., Zhang, Y., Zhao, H., Deng, Y., Yuan, W., *et al*. (2007) Microarray Analyses of Differentially Expressed Human Genes and Biological Processes in ECV304 Cells Infected with Rubella Virus. *Journal of Medical Virology*, **79**, 1783-1791. https://doi.org/10.1002/jmv.20942

[11] Zhang, Y., Ma, W., Mo, X., Zhao, H., Zheng, H., Ke, C., *et al*. (2014) Differential Expressed Genes in ECV304 Endothelial-Like Cells Infected with Human Cytomegalovirus. *African Health Sciences*, **13**, 864-879. https://doi.org/10.4314/ahs.v13i4.2

[12] Ramesh, P., Veerappapillai, S. and Karuppasamy, R. (2021) Gene Expression Profiling of Corona Virus Microarray Datasets to Identify Crucial Targets in COVID-19 Patients. *Gene Reports*, **22**, Article 100980. https://doi.org/10.1016/j.genrep.2020.100980

[13] Zhang, X., Tang, Q. and Xu, L. (2014) Herpes Simplex Virus 2 Infects Human Endothelial ECV304 Cells and Induces Cell Apoptosis Synergistically with ox-LDL. *The Journal of Toxicological Sciences*, **39**, 909-917. https://doi.org/10.2131/jts.39.909

[14] Mo, X., Xu, L., Yang, Q., Feng, H., Peng, J., Zhang, Y., *et al*. (2011) Microarray Profiling Analysis Uncovers Common Molecular Mechanisms of Rubella Virus, Human Cytomegalovirus, and Herpes Simplex Virus Type 2 Infections in ECV304 Cells. *Current Molecular Medicine*, **11**, 481-488. https://doi.org/10.2174/156652411796268696

[15] Streicher, J.M. (2019) The Role of Heat Shock Proteins in Regulating Receptor Signal Transduction. *Molecular Pharmacology*, **95**, 468-474. https://doi.org/10.1124/mol.118.114652

[16] Whitesell, L. and Dai, C. (2005) HSP90: A Rising Star on the Horizon of Anticancer Targets. *Future Oncology*, **1**, 529-540. https://doi.org/10.2217/14796694.1.4.529

[17] Torronteguy, C., Frasson, A., Zerwes, F., Winnikov, E., da Silva, V.D., Ménoret, A., *et al*. (2006) Inducible Heat Shock Protein 70 Expression as a Potential Predictive Marker of Metastasis in Breast Tumors. *Cell Stress & Chaperones*, **11**, 34.-43 https://doi.org/10.1379/csc-159r.1

[18] Gupta, A., Bansal, A. and Hashimoto-Torii, K. (2020) HSP70 and HSP90 in Neurodegenerative Diseases. *Neuroscience Letters*, **716**, Article 134678. https://doi.org/10.1016/j.neulet.2019.134678

[19] de Maio, A. (2014) Extracellular Hsp70: Export and Function. *Current Protein & Peptide Science*, **15**, 225-231. https://doi.org/10.2174/1389203715666140331113057

[20] Forouzanfar, F., Butler, A.E., Banach, M., Barreto, G.E. and Sahbekar, A. (2018) Modulation of Heat Shock Proteins by Statins. *Pharmacological Research*, **134**, 134-144. https://doi.org/10.1016/j.phrs.2018.06.020

[21] Kim, K. (2015) Interaction between HSP 70 and Inos in Skeletal Muscle Injury and Repair. *Journal of Exercise Rehabilitation*, **11**, 240-243. https://doi.org/10.12965/jer.150235

[22] Jiang, X., Prabhakar, A., Van der Voorn, S.M., Ghatpande, P., Celona, B., Venkataramanan, S., *et al*. (2021) Control of Ribosomal Protein Synthesis by the Microprocessor Complex. *Science Signaling*, **14**, eabd2639. https://doi.org/10.1126/scisignal.abd2639

[23] Baßler, J. and Hurt, E. (2019) Eukaryotic Ribosome Assembly. *Annual Review of Biochemistry*, **88**, 281-306. https://doi.org/10.1146/annurev-biochem-013118-110817

[24] Xia, C., Braunstein, Z., Toomey, A.C., Zhong, J. and Rao, X. (2018) S100 Proteins as an Important Regulator of Macrophage Inflammation. *Frontiers in Immunology*, **8**, Article 1908. https://doi.org/10.3389/fimmu.2017.01908

[25] Donato, R. (2001) S100: A Multigenic Family of Calcium-Modulated Proteins of the Ef-Hand Type with Intracellular and Extracellular Functional Roles. *The International Journal of Biochemistry & Cell Biology*, **33**, 637-668. https://doi.org/10.1016/s1357-2725(01)00046-2

[26] Leśniak, W., Jezierska, A. and Kuźnicki, J. (2000) Upstream Stimulatory Factor Is Involved in the Regulation of the Human Calcyclin (S100A6) Gene. *Biochimica et Biophysica Acta* (*BBA*)—*Gene Structure and Expression*, **1517**, 73-81. https://doi.org/10.1016/s0167-4781(00)00259-1

[27] Ilg, E.C., Schäfer, B.W. and Heizmann, C.W. (1996) Expression Pattern of S100 Calcium-Binding Proteins in Human Tumors. *International Journal of Cancer*, **68**, 325-332. https://doi.org/10.1002/(sici)1097-0215(19961104)68:3<325::aid-ijc10>3.0.co;2-7

[28] Briones-Orta, M.A., Avendaño-Vázquez, S.E., Aparicio-Bautista, D.I., Coombes, J.D., Weber, G.F. and Syn, W. (2017) Osteopontin Splice Variants and Polymorphisms in Cancer Progression and Prognosis. *Biochimica et Biophysica Acta* (*BBA—Reviews on Cancer*, **1868**, 93-108. https://doi.org/10.1016/j.bbcan.2017.02.005

[29] Qi, L., Basset, C., Averseng, O., Quéméneur, E., Hagège, A. and Vidaud, C. (2014) Characterization of Uo22+binding to Osteopontin, a Highly Phosphorylated Protein: Insights into Potential Mechanisms of Uranyl Accumulation in Bones. *Metallomics*, **6**, 166-176. https://doi.org/10.1039/c3mt00269a

[30] Hoskins, R., Hajnal, A.F., Harp, S.A. and Kim, S.K. (1996) The c. Elegans Vulval Induction Gene Lin-2 Encodes a Member of the MAGUK Family of Cell Junction Proteins. *Development*, **122**, 97-111. https://doi.org/10.1242/dev.122.1.97

[31] V. Barnabas, R. and Celum, C. (2012) Infectious Co-Factors in HIV-1 Transmission Herpes Simplex Virus Type-2 and HIV-1: New Insights and Interventions. *Current HIV Research*, **10**, 228-237. https://doi.org/10.2174/157016212800618156

[32] Qu, J., Zhou, Y., Li, Y., Yu, J. and Wang, W. (2021) CASK Regulates Notch Pathway and Functions as a Tumor Promoter in Pancreatic Cancer. *Archives of Biochemistry and Biophysics*, **701**, Article 108789. https://doi.org/10.1016/j.abb.2021.108789

[33] Liu, X., Qin, H., Liu, Y., Ma, J., Li, Y., He, Y., *et al*. (2024) The Biological Functions and Pathological Mechanisms of CASK in Various Diseases. *Heliyon*, **10**, e28863. https://doi.org/10.1016/j.heliyon.2024.e28863

[34] Becker, M., Mastropasqua, F., Reising, J.P., Maier, S., Ho, M., Rabkina, I., *et al*. (2020) Presynaptic Dysfunction in Cask-Related Neurodevelopmental Disorders. *Translational Psychiatry*, **10**, Article No. 312. https://doi.org/10.1038/s41398-020-00994-0

Abbreviations

HSV	Herpes simplex virus
AS	Atherosclerosis
ECV-304 cells	Human umbilical vein endothelial cells
HSV-2	Herpes simplex virus type 2
RP	Ribosomal proteins
CASK	Calcium/calmodulin-dependent serine protein kinase